Statistical modeling of the radio-frequency signal for partially and fully developed speckle based on a Generalized Gaussian model with application to echocardiography

Olivier Bernard, Basma Touil, Jan D'hooge, *Member, IEEE*,
and Denis Friboulet, *Member, IEEE*

Abstract

We have shown in a previous paper [1] that the statistics of the radio-frequency (RF) signals may be faithfully modelled through the so-called K_{RF} distribution, in situations ranging from fully to partially-developed speckle. We demonstrate in this paper that the Generalized Gaussian provides a reliable and computationally convenient approximation of the K_{RF} . The performance of the parameters estimators for the two distributions is evaluated and compared in terms of their bias and variance through numerical simulations. This framework is applied to the modeling of echocardiographic data. The ability of the Generalized Gaussian to model RF signals from cardiac tissues (myocardium) and blood regions is demonstrated on data acquired in vivo.

I. INTRODUCTION

Characterizing the statistics of the backscattered signal through reliable models is an important issue in medical ultrasound image analysis. In the field of echocardiographic imaging alone, this statistical modeling is a major component for classification [2], denoising [3] or segmentation [4], [5], [6], [7] tasks.

O. Bernard, B. Touil and D. Friboulet are with CREATIS, INSA, UCB, CNRS UMR 5220, Inserm U630, Building Blaise Pascal, 7 avenue Jean Capelle, 69621 Villeurbanne Cedex, France (e-mail: bernard@creatis.insa-lyon.fr).

J. Dhooge is with Cardiac Imaging Research, Department of Cardiology and Department of Electronic Engineering, Leuven, Belgium.

In imaging situations ranging from fully to partially-developed speckle, the statistics of the backscattered envelope signal may be described through the now well-known K distribution model [8], [9]. We have recently shown [1] that the statistics of the RF signal is then given by the so-called K_{RF} distribution and that this distribution can be applied to the modeling of echocardiographic data corresponding to blood (fully developed speckle) or myocardial regions (partially-developed speckle). While the K_{RF} has a clear physical basis (*i.e.* assumption of a uniform distribution of scatterers having K-distributed amplitudes), its practical use for characterization or segmentation tasks is however limited: as detailed in Section II, numerical simulations indeed show that the estimation bias and variance grow rapidly as the shape parameter increases, yielding unstable estimates in blood regions [1].

We propose in this work to model the statistics of the RF signal by using the Generalized Gaussian distribution, which has a simple expression and whose parameters can be estimated through closed-form Maximum Likelihood estimators. In this framework, we show that the Generalized Gaussian provides a reasonable approximation of the K_{RF} and demonstrate its ability to reliably model RF signals from echocardiographic data acquired in vivo. Early versions of this approach appeared in [11], [12].

This paper is structured as follows. We give in Section II the properties of the Generalized Gaussian model which motivate its use as a model for RF signal in the case of partially and fully developed speckle. The consistency of parameter estimation for the K_{RF} and the Generalized Gaussian distributions are then compared from numerical simulations. In Section III, the ability of the Generalized Gaussian to model RF signals from cardiac tissues and blood pools is evaluated from echocardiographic data acquired in vivo. The main conclusions are given in Section IV.

II. GENERALIZED GAUSSIAN MODEL FOR THE RADIO-FREQUENCY SIGNAL

A. The K_{RF} model

The K_{RF} model is based on the assumption that the scatterers present inside the system resolution cell are uniformly distributed and that their amplitude follow a K distribution. The statistics of a random variable distributed according to a K_{RF} distribution is described by the following probability density function (see [1] for details):

$$f_X(x) = \frac{b}{\sqrt{\pi}\Gamma(\nu)}\left(\frac{b\,|x|}{2}\right)^{\nu-0.5} K_{\nu-0.5}\left(b\,|x|\right) \tag{1}$$

---

[1]It is to be noted that this behavior is shared by the K-distribution when estimation is performed from the envelope signal [10]

where Γ is the Gamma function and $K_{\nu-0.5}$ is the modified Bessel function of the second kind of order $\nu - 0.5$. This expression is completely specified by its two parameters ν and b, such that ν controls the shape and b the scale of the pdf. Two particular cases for ν are to be noted (see Appendix A):

- the K_{RF} tends to a Gaussian as $\nu \to \infty$
- the K_{RF} is equal to a Laplacian distribution when $\nu = 1$

More generally, the K_{RF} yields a heavy tail distribution with a sharp peak when ν takes small values, whereas it approaches a Gaussian distribution as ν takes large values. As a consequence, large values of ν are well adapted to the modelling of fully developed speckle while small values of ν are associated to partially developed speckle. A few sample plots of the pdf for different parameters ν are shown in Fig. 1.

Several estimators may be devised to compute the shape parameter ν from data samples. We have shown in [1] that the so-called implicit estimator was the most consistent and it is therefore used in this study.

B. The Generalized Gaussian model

From the observation that fully speckle situations correspond to a Gaussian pdf and non-fully speckle situations yields heavy tail, Laplacian-like distribution (see Fig.1), we propose to approximate the K_{RF} distribution by the Generalized Gaussian (G.G.) distribution whose expression is:

$$g_X(x) = \frac{\beta}{2\alpha\Gamma\left(1/\beta\right)} exp\left(-\left(\frac{|x|}{\alpha}\right)^\beta\right) \tag{2}$$

β and α are the two parameters of the distribution where β controls the shape and α the scale of the pdf.

The Generalized Gaussian distribution has already been employed for noise modeling in optical image analysis [13], [14], wavelet coefficient statistical modeling [15] and recently in radar domain [16]. This noise model is commonly used in statistical studies since it captures the heavy tailed behavior that is often exhibited by real noise distributions. In ultrasound imaging, the Generalized Gaussian distribution appears as a good candidate to characterize the statistics of the RF signal for both fully and partially developed speckle situations for the following reasons:

- The K_{RF} distribution with parameter $\nu = 1$ is identical to a Generalized Gaussian distribution with shape parameter $\beta = 1$. For this particular situation, the two distributions are indeed equal to a Laplacian distribution;

- The K_{RF} distribution with parameter $\nu \to \infty$ is identical to a Generalized Gaussian distribution with shape parameter $\beta = 2$. For this particular situation, the two distributions are equal to a Gaussian distribution.

The estimation of the Generalized Gaussian parameters can be easily done using the Maximum Likelihood method, in which the set of parameters that maximizes the likelihood function is determined. Given n independent realizations $\{y_1, y_2, \cdots, y_n\}$ from a Generalized Gaussian density (with parameters β and α), the ML estimates of the parameters ($\hat{\beta}$ and $\hat{\alpha}$, respectively) satisfy the following relation [17]:

$$\begin{cases} 1 + \dfrac{\Psi(1/\hat{\beta})}{\hat{\beta}} - \dfrac{\sum_{i=1}^{n} log\left(|y_i|\right) \cdot |y_i|^{\hat{\beta}}}{\sum_{i=1}^{n} |y_i|^{\hat{\beta}}} + \dfrac{log\left(\frac{\hat{\beta}}{n} \sum_{i=1}^{n} |y_i|^{\hat{\beta}}\right)}{\hat{\beta}} = 0 & (3) \\ \hat{\alpha} = \left(\dfrac{\hat{\beta}}{n} \sum_{i=1}^{n} |y_i|^{\hat{\beta}}\right)^{\frac{1}{\hat{\beta}}} & (4) \end{cases}$$

where $\Psi(.)$ is the digamma function. From equation (3) the parameters estimates are obtained using a bisection method.

C. Parameters estimation consistency

As mentioned in the introduction, one practical limitation of the K_{RF} is that the associated parameter estimators yield large bias and variance, particularly in the case of fully developed speckle situation. The consistency of parameter estimation for the K_{RF} and the Generalized Gaussian distributions has thus been investigated. Data distributed according to the K_{RF} distribution and the Generalized Gaussian have been generated and parameter estimation has been performed as follows:

- K_{RF} : Data were generated for values of the shape parameter ν in the range $[0.2, 10]$, which encompass the range observed from in vivo echocardiographic data, where ν was found to vary between 0.2 and 1.3 for myocardial regions (partially-developed speckle situation) and to be higher than 2 in blood regions (fully developed speckle situation). The implicit estimator mentioned in section II-A was used to evaluate ν.

- Generalized Gaussian : Data were generated for values of the shape parameter in the range $[0.6, 2]$, which encompass the range observed from in vivo echocardiographic data, where β was found to vary between 0.6 and 1.2 for myocardial regions and to be in the range $[1.5, 1.9]$ for blood regions. The ML estimator given in (3) was used.

The number of data samples (N) was chosen to be 1024 and the procedure was repeated 20000 times. The corresponding bias and variance are presented in Fig. 2. The results clearly show that the

Generalized Gaussian estimator has a better consistency than the K_{RF} estimator for the range of values corresponding to myocardium and blood regions. In particular, it may be observed that the estimator variance grows rapidly for the K_{RF} when the shape parameter increases. Moreover, it is interesting to note that for $\nu = 1$ (*i.e.* when the K_{RF} distribution is equal to the Generalized Gaussian distribution with parameter $\beta = 1$), the bias of the Generalized Gaussian estimator is 4 times lower than the bias corresponding to the K_{RF} estimator (the bias values are 0.012 and 0.049 for the Generalized Gaussian and the K_{RF} respectively). In this case, the variance of the Generalized Gaussian estimator is 5 times lower than the variance corresponding to the K_{RF} estimator (the variance values are 0.0034 and 0.02 for the Generalized Gaussian and the K_{RF} respectively). These results illustrates the interest of using the Generalized Gaussian distribution as an approximation of the K_{RF} distribution.

III. EXPERIMENTAL RESULTS

We tested the ability of the two distributions to model RF data on a variety of ultrasound cardiac images of clinical interest using the same protocol as in [1]. Data were acquired using a Toshiba Powervision 6000 (Toshiba Medical Systems Europe, Zoetermeer, The Netherlands) equipped with an RF interface for research purposes and a 3.75-MHz probe. The RF signal was acquired without any attenuation correction. The RF sample frequency varied between 25 and 32 MHz according to the acquisition mode. Table I summarizes the various image orientations and the corresponding left ventricular segments used in the experiments. For each view, five independent RF data sets (from five different, healthy volunteers) were acquired, from which a single image was selected visually to provide easy discrimination between the myocardium region and the blood pool. Subsequently, a trained cardiologist manually drew a contour delimiting a region inside the myocardium and a region inside blood pool (Fig. 3 give examples of myocardial regions obtained for each view). In each region, the fit of the K_{RF} and the Generalized Gaussian distributions was done from the corresponding RF data. The fits were obtained using the implicit and the ML methods for estimating the parameters of the K_{RF} and Generalized Gaussian distributions, respectively. The sample size was chosen to be equal to 1024 in each region.

The ability of the distributions to model the RF data was expressed through the root mean square error (RMSE) and a goodness-of-fit measure. The latter was measured through a Chi-square (χ_2)-type test. As the conventional χ_2 test, based on the Pearson's measure, is heavily affected by small, expected frequencies that commonly appear when dealing with heavy tail distributions such as K_{RF} or Generalized Gaussian , we used the χ_2 Freeman-Tukey measure (FT) instead [1]. The number of bins used to build the histograms from the data was selected according to the approach proposed by D'Agostino and Stephens

[1] by setting $M = 2n^{2/5}$, where M is the number of bins and n is the sample size. The test associated to FT also enables us to accept or reject the hypothesis that a particular distribution could model the empirical data for a chosen level of significance.

Table II(a) and II(b) show the average RMSE and FT goodness of fit measures for each of the two distributions for each image view, respectively for blood and myocardial regions. Table II(a) shows that for blood regions, the K_{RF} and Generalized Gaussian distributions provide almost the same fit for each image orientation. The value of the shape parameter is in the range $[1.9, 89.4]$ for the K_{RF} and in the range $[1.5, 1.9]$ for the Generalized Gaussian model. This shows that the two distributions are close to a Gaussian. This observation is consistent with the fact that blood areas corresponds to fully developed speckle. Table II(b) shows that for myocardial regions, the Generalized Gaussian distribution provides slightly better fits than the K_{RF} model for each image orientation. The value of the shape parameter is in the range $[0.2, 1.3]$ for the K_{RF} and in the range $[0.6, 1.2]$ for the Generalized Gaussian model.

Finally the FT test was undertaken with a significance level of 0.01 to accept or reject the K_{RF} or Generalized Gaussian hypothesis on the 40 studied cases. Results show that the acceptation rate was 24 for the K_{RF} and 29 for the Generalized Gaussian . Here again, the Generalized Gaussian performs slightly better than the K_{RF} . In order to illustrate more qualitatively the above results we give in Fig. 4 fits of the distributions to the empirical RF data for two opposite situations. Fig. 4(a) shows a result obtained for a case where the goodness of fit measure was low and the FT test succeeded. Fig. 4(b) shows a result for a case where the goodness of fit measure was high and the FT test failed. Fig. 4(a)-(b) illustrates again that the Generalized Gaussian provides a reliable approximation of the K_{RF} distribution.

IV. Conclusion

In this work, we have proposed to model the statistics of the radio-frequency signal in the case of both fully and partially developed speckle using the Generalized Gaussian distribution. We demonstrated that the statistical distribution derived from the modeling of the scattering configuration (K_{RF} distribution) can be reasonably approximated by the Generalized Gaussian distribution. This distribution has the advantage to have a simple expression with consistent parameters estimation. The experimental results clearly show the reliability and versatility of this distribution in representing RF data corresponding to partially developed speckle (myocardial regions) and fully developed speckle (blood regions).

APPENDIX A

RELATION BETWEEN K_{RF} AND GENERALIZED GAUSSIAN DISTRIBUTIONS

From equation (2), it is easily seen that the Gaussian and the Laplacian distributions can be viewed as particular cases of the Generalized Gaussian model for shape parameter β value 2 and 1, respectively. In this appendix, we show that these two distributions are also special cases of the K_{RF} model.

A. Gaussian case

The fact that the K_{RF} pdf $f_X(x)$ tends to a Gaussian distribution is easily demonstrated using the basic properties of the K distribution. Let us call $Kd\,_U^{\nu,b}(u)$ a K distribution with shape parameter ν and scale parameter b. $Kd\,_U^{\nu,b}(u)$ tends to a Rayleigh distribution as ν tends to infinity [8], that is

$$\lim_{\nu \to \infty} Kd\,_U^{\nu,b}(u) = \frac{u}{\sigma^2} \exp\left(-\frac{u^2}{2\sigma^2}\right) \tag{5}$$

Let $P_{X,Y}(x,y)$ be the pdf of the analytic form of the RF signal $x + iy$. $P_{X,Y}(x,y)$ may be expressed as a function of a K distribution pdf as [1]:

$$P_{X,Y}(x,y) = \frac{1}{2\pi z} Kd\,_Z^{\nu,b}(z) \qquad \text{where} \qquad z = \sqrt{x^2 + y^2} \tag{6}$$

From (5) and (6) it follows immediately that $P_{X,Y}(x,y)$ tends to a circular Gaussian distribution as ν tends to infinity.

The RF signal corresponds to the real part of the analytic signal, so the K_{RF} corresponds to the marginal distribution obtained by integrating of $P_{X,Y}(x,y)$ with respect to y. When ν tends to infinity, the K_{RF} thus tends to a Gaussian distribution.

B. Laplacian case

For the special case of $\nu = 1$, the K_{RF} expression given in (1) is equal to:

$$f_X(x) = \frac{b}{\sqrt{\pi}} \frac{\sqrt{b}\sqrt{|x|}}{\sqrt{2}} K_{1/2}\left(b\,|x|\right) \tag{7}$$

Noting that

$$K_{1/2}(u) = \sqrt{\frac{\pi}{2}} \frac{\exp(-u)}{\sqrt{u}} \tag{8}$$

We obtain

$$f_X(x) = \frac{b}{2} \exp\left(-b\,|x|\right) \tag{9}$$

which corresponds to a Laplacian density with mean value equal to zero and shape parameter equal to $1/b$

REFERENCES

[1] O. Bernard, J. D'hooge, and D. Friboulet, "Statistics of the radio-frequency signal based on k distribution with application to echocardiographic images," *IEEE Trans. Ultrason., Ferroelect., Freq. Contr.*, vol. 53, no. 9, pp. 1689–1694, 2006.

[2] P. Shankar, "Ultrasonic tissue characterization using a generalized nakagami model," *IEEE Trans. Ultrason., Ferroelect., Freq. Contr.*, vol. 48, pp. 1716–20, 2001.

[3] V. Dutt and J. Greenleaf, "Adaptive speckle reduction filter for log-compressed b-scan images," *IEEE Trans. Biomed. Eng.*, vol. 15, no. 6, pp. 802–813, 1996.

[4] M. Mignotte and J. Meunier, "A multiscale optimization approach for the dynamic contour-based boundary detection issue," *Comput. Med. Imag. Graph.*, vol. 25, no. 3, pp. 265–275, 2001.

[5] D. Boukerroui, A. Baskurt, J. Noble, and O. Basset, "Segmentation of ultrasound images-multiresolution 2d and 3d algorithm based on global and local statistics," *Pattern Recognition Lett.*, vol. 24, pp. 779–790, 2003.

[6] A. Sarti, C. Corsi, E. Mazzini, and C. Lamberti, "Maximum likelihood segmentation of ultrasound images with rayleigh distribution," *IEEE Trans. Ultrason., Ferroelect., Freq. Contr.*, vol. 41, no. 4, pp. 435–440, 2005.

[7] I. Dydenko, F. Jamal, O. Bernard, J. Dhooge, I. Magnin, and D. Friboulet, "A level set framework with a shape and motion prior for segmentation and region tracking in echocardiography," *Medical Image Analysis*, vol. 10, no. 2, pp. 162–177, 2006.

[8] P. Shankar, "A model for ultrasonic scattering from tissues based on the k distribution," *Phys. Med. Biol.*, vol. 40, pp. 1633–1649, 1995.

[9] L. Clifford, P. Fitzgerald, and D. James, "Non-rayleigh first-order statistics of ultrasonic backscatter from normal myocardium," *Ultrasound in Medicine and Biology*, vol. 19, no. 6, pp. 487–495, 1993.

[10] D. D. Blacknell and R. Tough, "Parameter estimation for the k-distribution based on [z log(z)] iee proc. radar, sonar and navigation," in *IEE Proc. Radar, Sonar and Navigation*, vol. 146, no. 6, 2001, pp. 309–312.

[11] O. Bernard, J. D'hooge, and D. Friboulet, "Segmentation of echocardiographic images based on statistical modelling of the radio-frequency signal," in *IEEE International Symposium on Biomedical Imaging*, Washington, USA, 2006, pp. 153–156.

[12] ——, "Statistical modeling of the radio-frequency signal in echocardiographic images using modified k-distribution and generalized gaussian distribution," in *IEEE International Ultrasonics Symposium*, Vancouver, Canada, 2006, p. in press.

[13] C. Bouman and K. Sauer, "A generalized gaussian image model for edge-preserving map estimation," *IEEE Trans. Image Process.*, vol. 2, no. 3, pp. 296–310, 1993.

[14] P. Moulin and J. Liu, "Analysis of multiresolution image denoising schemes using generalized gaussian and complexity priors," *IEEE Trans. Inf. Theory*, vol. 45, no. 3, pp. 909–919, 1999.

[15] S. Mallat, "A theory of multiresolution signal decomposition: the wavelet representation," *IEEE Trans. Patt. Anal. Mach. Intell.*, vol. 11, pp. 674–693, 1989.

[16] G. Moser, J. Zerubia, and S. B. Serpico, "Sar amplitude probability density function estimation based on a generalized gaussian model," *IEEE Transactions on Image Processing*, vol. 15, no. 6, pp. 1429–1442, 2006.

[17] S. Meignen and H. Meignen, "On the modeling of small sample distributions with generalized gaussian density in a maximum likelihood framework," *IEEE Transactions on Image Processing*, vol. 15, no. 6, pp. 1647–1652, 2006.

TABLE I

Orientation	Processed tissue area
Apical four chambers (AP4CH)	Interventricular septum
Apical two chambers (AP2CH)	Left ventricle anterior wall
Parasternal long axis (PALA)	Left ventricle inferolateral wall
Parasternal short axis (PASA)	Left ventricle inferolateral wall

TABLE II

Blood				
Orientation	RMSE measure		Freeman-Tukey measure	
	K_{RF}	G.G.	K_{RF}	G.G.
AP4CH	5.4	5.5	24.2	24.8
AP2CH	4.4	4.5	22.3	22.4
PALA	5.0	5.1	25.3	26.2
PASA	5.7	5.8	23.8	24.5

(a)

Tissue				
Orientation	RMSE measure		Freeman-Tukey measure	
	K_{RF}	G.G.	K_{RF}	G.G.
AP4CH	13.3	5.8	51.2	23.5
AP2CH	10.8	6.7	44.4	32.6
PALA	15.1	8.4	63.1	26.2
PASA	17.7	6.3	69.9	28.3

(b)

Figure 1: K_{RF} pdf for several values of parameter ν : $\{0.75, 1.5, 4, 20\}$. The smaller the parameter ν value, the sharper the curve. The curves were normalized so that the mean square value of the pdfs is unity.

Figure 2: Comparison of the estimated Bias and Sample Variance of ν and β using the implicit and Maximum Likelihood estimator using $N = 1024$ for the K_{RF} and the Generalized Gaussian distributions respectively. Note that the bias and variance are given on a logarithmic scale. (a) : Bias of ν (K_{RF}). (b) : Bias of β (Generalized Gaussian). (c) : Variance of ν (K_{RF}). (d) : Variance of β (Generalized Gaussian).

Figure 3: Examples of myocardial regions used for the tests (a): Apical four chambers (AP4CH). (b): Apical two chambers (AP2CH). (c): Parasternal long axis (PALA). (d): Parasternal short axis (PASA).

Figure 4: Fitting probability density function to empirical data for two opposite situations. (a): A case where the goodness of fit measure was low and the FT test succeeded. The FT measures were 17.4 and 16.9 for the K_{RF} and Generalized Gaussian distributions, respectively, and the threshold for the test was 27.7. (b): A case where the goodness of fit measure was high and the FT test failed. The FT measure were 76.7 and 52.1 for the K_{RF} and Generalized Gaussian distributions, respectively, and the threshold for the test was 33.4.
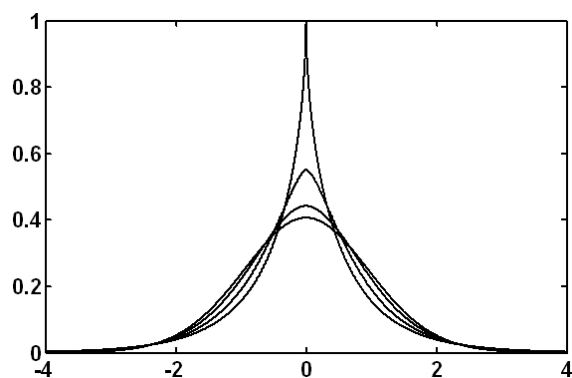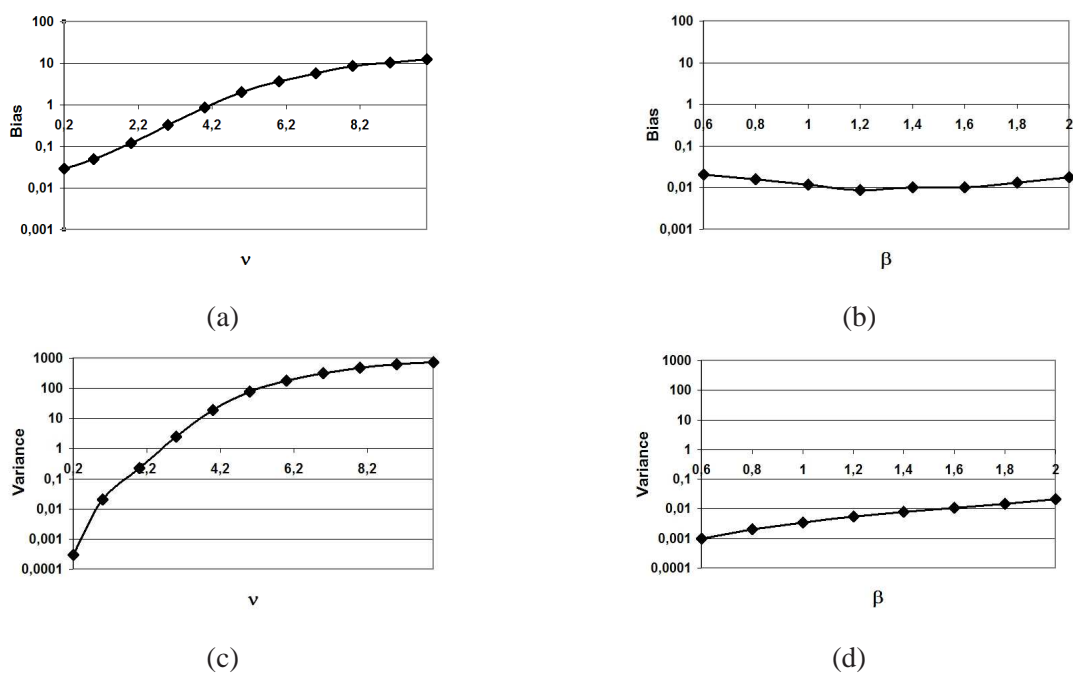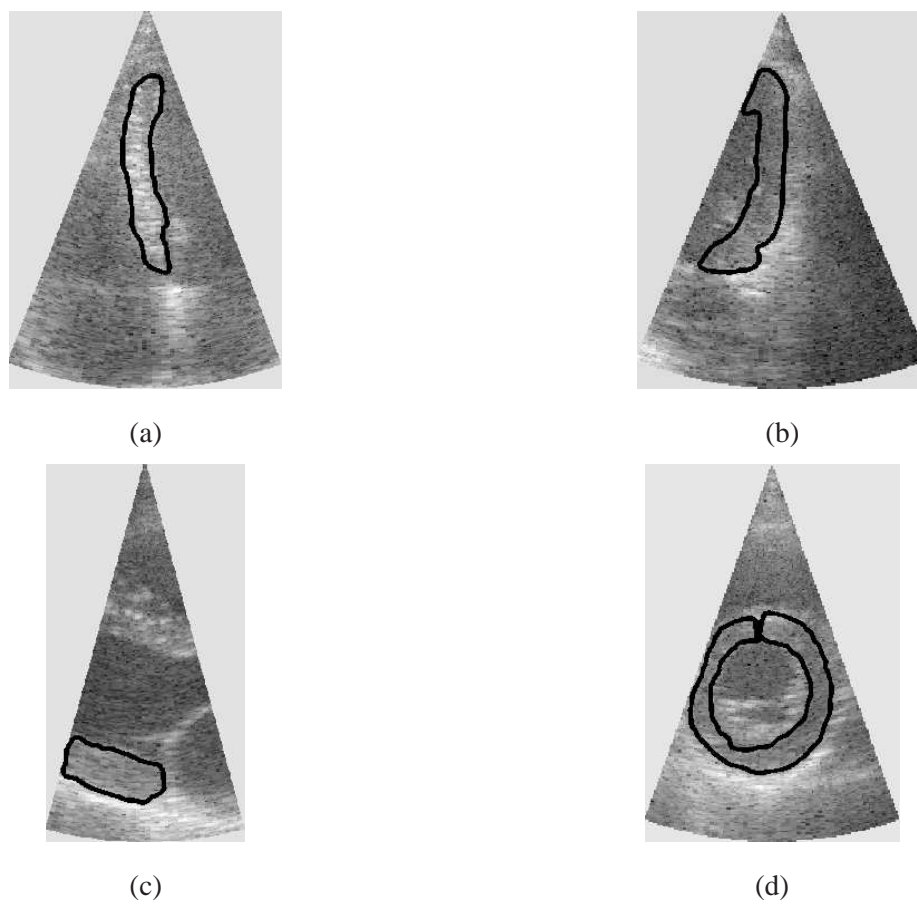
Fig. 1.

Fig. 2.

(a)

(b)

(c)

(d)

Fig. 3.

(a)

(b)

(c)

(d)

Fig. 4.

(a)

(b)